COMMUNICATION

Dielectrophoretically Aligned Carbon Nanotubes to Control Electrical and Mechanical Properties of Hydrogels to Fabricate Contractile Muscle Myofibers

Javier Ramón-Azcón, Samad Ahadian, Mehdi Estili, Xiaobin Liang, Serge Ostrovidov, Hirokazu Kaji, Hitoshi Shiku, Murugan Ramalingam, Ken Nakajima, Yoshio Sakka, Ali Khademhosseini, and Tomokazu Matsue**

Tissue engineering generally involves the proliferation and differentiation of cells within a scaffold that mimics the native extracellular matrix (ECM). Hydrogels are often used as scaffolds due to their high water content, biocompatibility, and biodegradability.[1,2] However, they generally have weak mechanical properties and low conductivity, which limit their application in regulating the behavior of electroactive cells, such as skeletal, cardiac, and neural cells.[3] Therefore, controlling the mechanical and electrical properties of hydrogels is desirable in regulating cell behaviors. Electrically conductive and mechanically strong hydrogels have other important applications, such as in real-time monitoring of cellular activities,[4,5] developing hybrid three-dimensional (3D) electronics-tissue materials,[6,7] and as bioactuators.[8]

Nanomaterials have recently gained much attention as tools to improve the electrical and mechanical properties of biomaterials.[9] For instance, alginate hydrogels impregnated with gold nanostructures improved the electrical conductivity and cellular excitability of both cardiomyocytes and neural cells.[3,10] Nanomaterials encapsulated in scaffold materials could also enhance sensitivity of engineered tissues mimicking the native nervous system,[11] which can be used in the fundamental cell biology and diagnostics. For example, carbon nanotubes (CNTs)[12] and nanowires[13] have been used to sense extra- and intra-cellular activity of cells or to tailor the delivery of therapeutic molecules to cells.

We have previously demonstrated that gelatin methacrylate (GelMA) hydrogels emulated the ECM for various cell types, such as that of muscle, cardiac, and endothelial cells.[14] GelMA is a photocrosslinkable hydrogel derived from natural gelatin. As recently reported, multi-walled carbon nanotubes (MWCNTs) can effectively reinforce GelMA hydrogels without negatively impacting cell behavior.[15] The formation of nanofiber web-like structures of CNTs within GelMA hydrogels enhanced the mechanical properties of GelMA-CNTs hybrid systems compared with the pure GelMA hydrogel.[15] However, despite unique electrical conductive properties of CNT, there has been no report to tune electrical properties of

Prof. A. Khademhosseini
Department of Medicine
Center for Biomedical Engineering
Brigham and Women's Hospital
Harvard Medical School
Cambridge, Massachusetts 02139, USA
Harvard–MIT Division of Health Sciences and Technology
Massachusetts Institute of Technology
Cambridge, Massachusetts 02139, USA
Wyss Institute for Biologically Inspired Engineering
Harvard University, Boston
Massachusetts 02115, USA
and Department of Maxillofacial Biomedical Engineering
and Institute of Oral Biology
School of Dentistry
Kyung Hee University
Seoul 130-701, Republic of Korea
E-mail: alik@rics.bwh.harvard.edu
Prof. H. Shiku, Prof. T. Matsue
Graduate School of Environmental Studies
Tohoku University
Sendai 980-8579, Japan
E-mail: matsue@bioinfo.che.tohoku.ac.jp

DOI: 10.1002/adma.201301300

Dr. J. Ramón-Azcón,[†] Dr. S. Ahadian,[†] Mr. X. Liang,
Prof. S. Ostrovidov, Prof. M. Ramalingam,
Prof. K. Nakajima, Prof. A. Khademhosseini,
Prof. T. Matsue
WPI-Advanced Institute for Materials Research
Tohoku University, Sendai 980-8577, Japan
Dr. M. Estili, Prof. Y. Sakka
Materials Processing Unit
National Institute for Materials Science (NIMS)
Tsukuba 305-0047, Japan
Prof. H. Kaji
Department of Bioengineering and Robotics
Graduate School of Engineering
Tohoku University
Sendai 980-8579, Japan
Prof. M. Ramalingam
Centre for Stem Cell Research
A unit of the Institute for Stem Cell Biology
and Regenerative Medicine
Christian Medical College Campus
Vellore 632002, India
Institut National de la Santé Et de la Recherche Médicale U977
Faculté de Chirurgie Dentaire
Université de Strasbourg, Strasbourg 67085, France
[†] These authors contributed equally to this work.

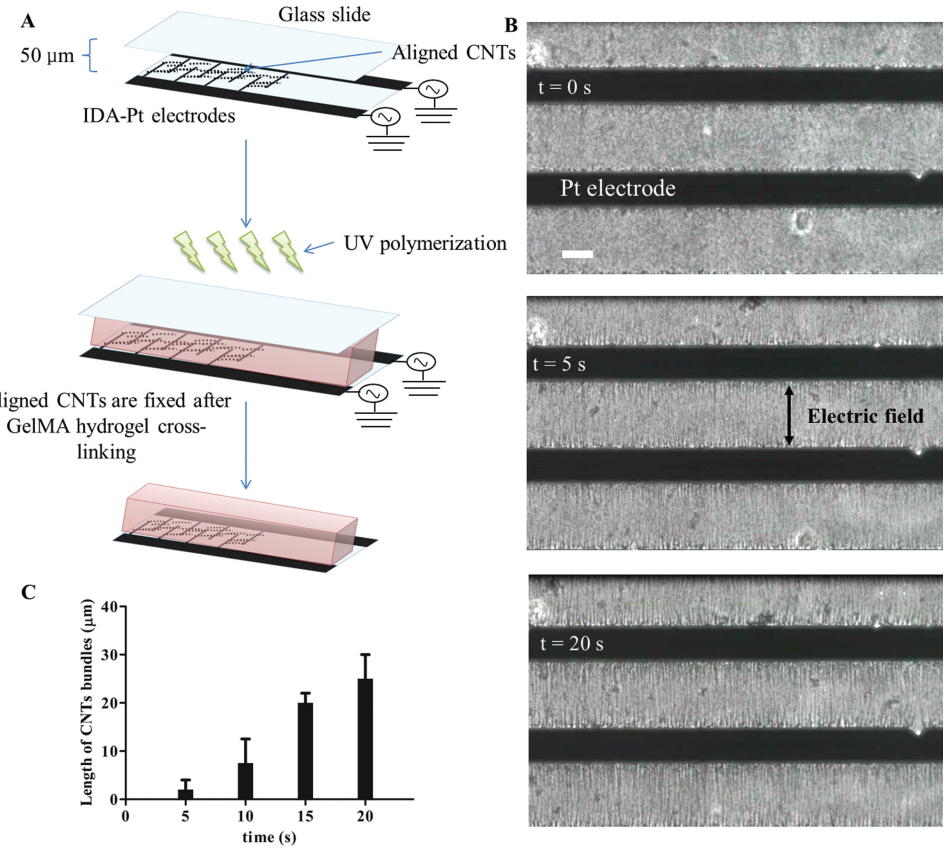

Figure 1. Process of the CNTs' alignment as bundles within the GelMA hydrogel under dielectrophoresis (DEP) force. (A) Schematic representation of the fabrication process for CNT alignment within the GelMA hydrogel. Dispersed CNTs' in the GelMA prepolymer were introduced into the 50-µm-height chamber and patterned by DEP forces (20 V and 2 MHz) within the electrodes. The chamber was then irradiated with UV light for 150 s. (B) Phase contrast images of the CNT alignment over time. CNTs were aligned after 20 seconds. (C) Length of CNT bundles over time. Scale bar shows 50 µm.

GelMA hydrogels using nanoscale alignment of CNTs. Here, we propose dielectrophoresis (DEP) as an enabling tool to pattern CNTs within GelMA hydrogels. DEP is a powerful technique to manipulate particles based on their responses to an AC electric field, which induces a charge polarization within the particles and their surrounding medium.[16,17] Due to the low ion concentration and viscosity of GelMA, we hypothesized that it would provide a suitable milieu for CNT alignment using DEP.

In this study, DEP was applied to obtain aligned CNTs within GelMA hydrogels. The electrical and mechanical features of GelMA-CNT hydrogels were quantified and compared with pristine GelMA hydrogels. To demonstrate the utility of these novel hydrogels, the GelMA and GelMA-CNT hydrogels were then used to fabricate C2C12 muscle myofibers and were characterized in terms of contractility of myotubes and gene expression related to muscle cell differentiation.

CNTs were initially functionalized with carboxyl groups to render them water-soluble. The CNTs exhibited cylindrical morphology; an aspect ratio greater than 100; and a wide diameter distribution (40–90 nm), as revealed by transmission electron microscope (TEM) and scanning electron microscope (SEM) images (see Supporting Information, Figure S1). The Raman spectra of CNTs (Figure S2) indicated that the CNTs were of high quality. Here, CNTs were coated and stabilized with a thin layer of GelMA hydrogel, as confirmed from our previous work.[15] The DEP approach was then used to pattern CNTs within the GelMA hydrogels, as shown in **Figure 1**. AC electric fields appeared to induce dipole moments within CNTs and forced them to align in the direction of the electric field. Note that the CNTs were attached together and aligned as the bundle in their axial direction. By adjusting voltages and frequencies, CNTs could be successfully aligned within GelMA hydrogels (using 2 MHz and 20 Vpp, respectively) by applying current through an interdigitated array of Pt (IDA-Pt) electrodes (see Supporting Information, Movie 1). Additional techniques can also pattern CNTs on or into biomaterials. For example, Sung et al. reported the use of electrospinning for the alignment of CNTs within poly(methyl methacrylate) (PMMA).[18] However, they observed that as the CNT concentration was increased to 5 wt%, the alignment of CNTs became irregular because of CNT aggregation during the electrospinning process. In general, CNT alignment within polymers using electrospinning does not appear to be robust, likely due to relaxation after fiber formation[19] and highly tangled electrospun hybrid CNT-polymers, leading to bent and twisted CNTs and agglomerate formation.[20–22] Another approach to achieve aligned CNTs within biomaterials is to apply mechanical strain to the hybrid

ADVANCED MATERIALS
www.advmat.de

www.MaterialsViews.com

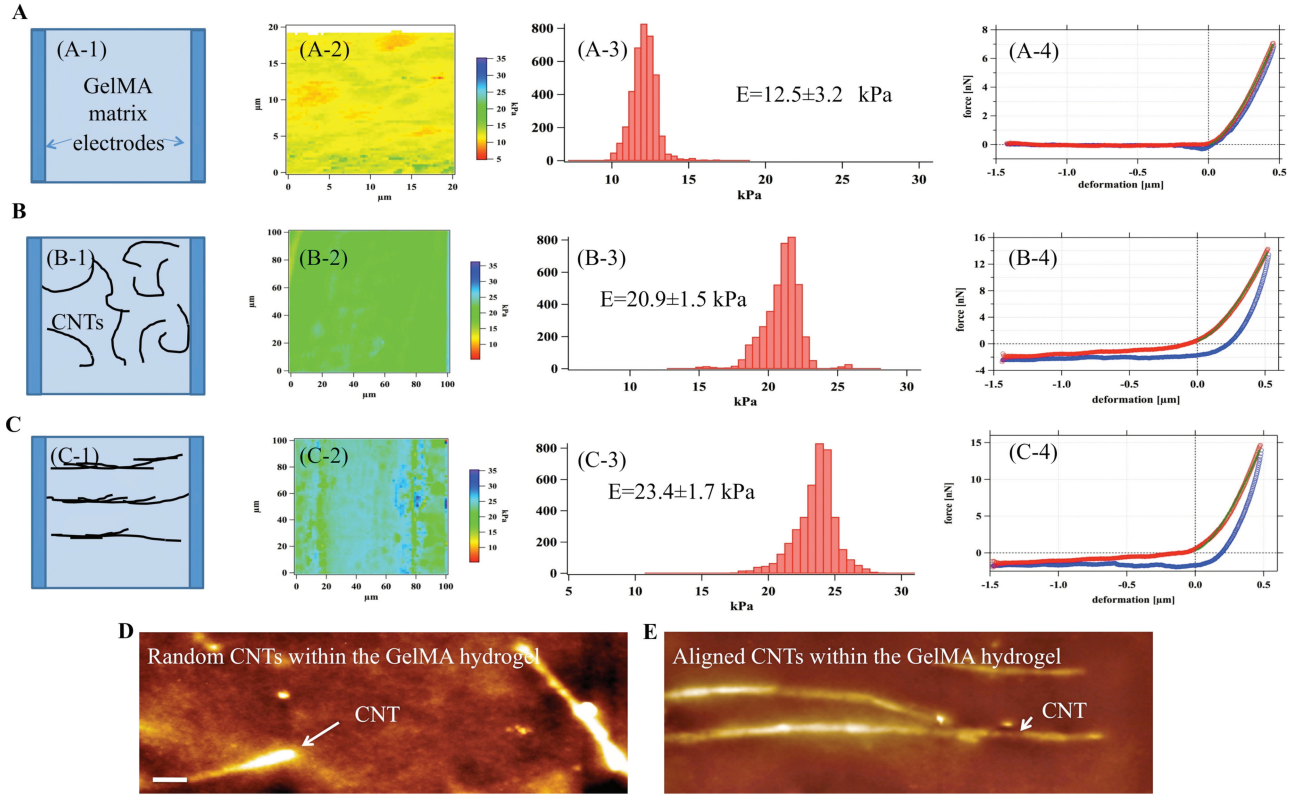

Figure 2. Mechanical and morphological properties of the 5% GelMA and aligned/non-aligned hybrid GelMA-CNT hydrogels (0.3 mg/mL CNTs), as measured by AFM. (A) Schematic representation, Young's modulus map and its histogram, and force deformation curves for the pure 5% GelMA hydrogel (A-1, A-2, A-3, and A-4, respectively). The red curve represents the force deformation curve as the AFM cantilever approached the surface, while the blue curve is the force deformation curve produced when the cantilever left the surface. The green line was calculated according to the DMT theory. (B) Schematic representation, Young's modulus map and its histogram, and force deformation curves of the CNTs randomly dispersed in the GelMA hydrogel (B-1, B-2, B-3, and B-4, respectively). (C) Schematic representation, Young's modulus map and its histogram, and force deformation curves of the CNTs aligned within the GelMA hydrogel (C-1, C-2, C-3, and C-4, respectively). (D) AFM picture of randomly dispersed CNTs within the 5% GelMA hydrogel. Scale bar is 200 nm. (E) AFM picture of the aligned CNTs embedded in the 5% GelMA hydrogel.

CNTs-biomaterials. Voge et al. used this approach to obtain aligned single-walled carbon nanotubes (SWCNTs) within collagen-fibrin hydrogels over the course of hours.[23] Their results showed that hydrogels with anisotropic CNTs had higher conductivity compared with hydrogels containing randomly dispersed CNTs. Individual CNTs were also aligned using a simple spinning technique.[24] However, using this approach, CNTs could only align in the radial direction. In contrast, the proposed DEP approach here provides facile, rapid, and reproducible alignment of CNTs within a scaffold material (i.e., GelMA hydrogel). The whole process took less than one minute (Movie S1). In addition, there was no destructive effect on the structure and morphology of CNTs, as confirmed by the assessment of atomic force microscopy (AFM) measurements of aligned CNTs after DEP and in the absence of an electric field (**Figure 2**-E and 2-D, respectively). Here, GelMA hydrogel polymerization is crucial for preserving aligned CNTs after removing the current. Figure 1-A to 1-C show CNTs aligned within the gaps of the IDA-Pt electrodes in less than one minute.

The hybrid GelMA-CNT hydrogels with CNTs concentrations of 0.1, 0.3, 1, and 2 mg/mL were prepared with and without CNTs alignment. The DC conductivity of all these structures was measured and compared with the conductivity of the pristine GelMA. Here, the IDA-Pt electrodes were used for the measurement of DC conductivity. As shown in **Figure 3**, the electrical conductivity along with the CNT alignment was dramatically increased as a function of CNT concentration. Most importantly, there was few orders of magnitude increase in conductivity as the CNTs were aligned within the GelMA hydrogel compared with randomly oriented CNTs within the GelMA. A similar trend was observed for impedance of the hydrogels (Figure 3-C). Impedance spectra were acquired for the GelMA and GelMA-CNT hydrogels on the IDA-Pt electrodes over a frequency range from 10 to 10^5 Hz with a perturbation amplitude of 25 mV. The same behavior was observed as we increased the perturbation amplitude to 1 V (Figure S3). The substantially higher conductivity of GelMA hydrogels with aligned CNTs compared with hydrogels with randomly oriented CNTs is most likely due to the formation of an intertwined CNT network through which the current could be passed.

In the present study, a micromechanical mapping technique was used to measure the mechanical properties of the nanostructured hybrid GelMA-CNTs gels, including elasticity and surface topography. The results, summarized in

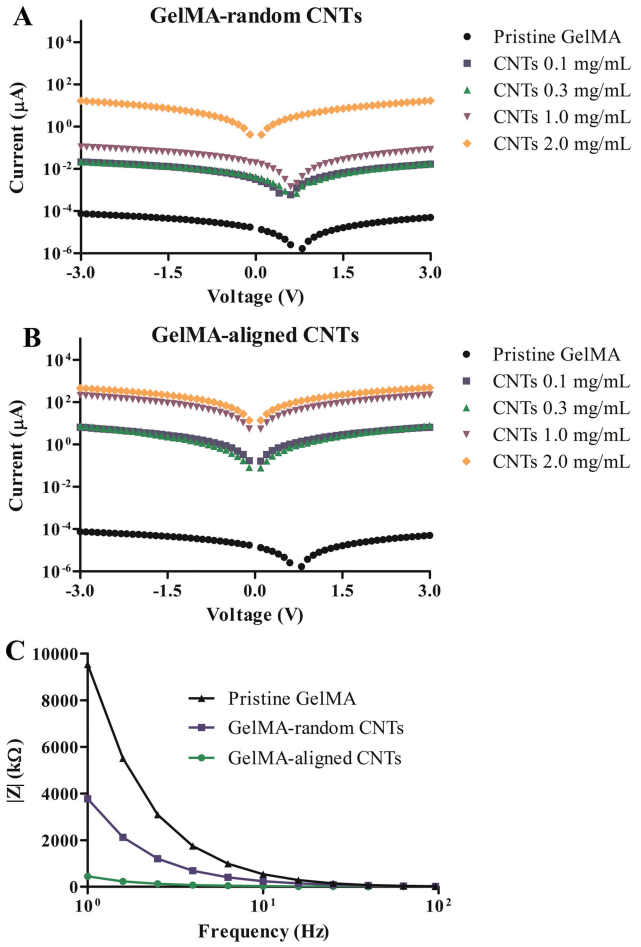

Figure 3. Conductivity of hybrid GelMA-CNT gels with different concentrations of CNTs, along with the pristine GelMA (i.e., 0 mg/mL CNTs). (A) *Current-Voltage* (*I–V*) curves for the pristine GelMA and for the GelMA hydrogels with randomly distributed CNTs. The CNT concentration was varied from 0.1 to 2.0 mg/mL. (B) I-V curves for the pristine GelMA and for the GelMA hydrogels with aligned CNTs. The CNT concentration was varied from 0.1 to 2.0 mg/mL. (C) Impedance measurements of the pristine GelMA and the hybrid gels loaded with 0.3 mg/mL CNTs. The perturbation amplitude was 25 mV.

Figure 2, show that Young's modulus for the pristine GelMA was 12.5 ± 0.09 kPa, which agrees with our previously reported value derived from conventional stress-strain measurements.[14] Because the GelMA was reinforced with 0.3 mg/mL CNTs, its Young's modulus increased to 20.9 ± 0.12 and 23.4 ± 0.17 kPa for the random and aligned CNTs within the GelMA hydrogel, respectively. This increase in Young's modulus was likely due to the formation of a well-connected 3D network structure within the hydrogel. CNT alignment most likely caused an extra reinforcement between the CNTs bundles. Therefore, there was a slight increase in Young's modulus for the aligned CNTs within the GelMA compared with the randomly oriented CNTs. Force deformation curves are shown in Figure 2-A-4, B-4, and C-4, taking into consideration one representative point of the corresponding Young's modulus maps. The Derjaguin, Muller, and Toporov (DMT) model[25] was used to generate the deformation plots. Interestingly, the pristine GelMA hydrogel exhibited a typical elastic deformation curve (Figure 2-A-4); however, the hybrid hydrogels showed a viscoelastic behavior with the addition of CNTs (Figure 2-B-4 and C-4), likely due to the viscoelastic behavior of the encapsulated CNTs. We further confirmed this result by measuring the elastic modulus and the force curve of 1 mg/mL aligned CNTs within the GelMA hydrogel (Figure S4). The mechanical properties of scaffolds affect cell behavior and fate, such as cell adhesion, proliferation, and differentiation.[26] Therefore, hydrogels with tunable mechanical properties are of great interest. A simple method to increase the compressive modulus of hydrogels is to decrease the water content of hydrogels. However, this method reduces the porosity and interconnectivity of hydrogels and has adverse effects on the performance of hydrogels.[14,27] For example, as shown in our recent work, increasing the compressive modulus of GelMA hydrogels by increasing the concentration of methacrylate limited cell viability and growth, morphogenesis, and cell migration.[28] In this regard, CNTs hold great potential as a supplementary material for scaffolds due to their extraordinary mechanical properties. GelMA hydrogels containing CNTs were shown viscoelastic behavior similar to soft tissue membranes[29]; therefore, they could be ideal scaffolds for soft tissues, such as skeletal muscle.

Encapsulated CNTs in GelMA at a concentration of 0.3 mg/mL significantly increased the electrical conductivity and moderately strengthened the mechanical properties. Therefore, this concentration was chosen for further skeletal muscle cell experiments. As reported in Figure S5, more than 95% of C2C12 myoblasts remained viable on both pristine GelMA and GelMA-CNT hydrogels and the difference between cell viability on the pristine GelMA and GelMA-CNT hydrogels was not significant. Similar results were obtained for cell proliferation, except that there was an increase in cell proliferation for the GelMA-CNT hydrogels compared with the pristine GelMA hydrogels on day 3 of culture. This difference may be caused by the increased elastic modulus and viscoelsticity of the hybrid gels. C2C12 myoblasts need a substrate to attach and proliferate. Here, it seems that hybrid GelMA-CNT hydrogels provide more anchoring sites for the cellular adhesion and proliferation compared with pristine GelMA hydrogels. As demonstrated in our previous works,[30,31] topological cues have a great impact on the morphological and unidirectional orientation of C2C12 myoblasts. A high degree of C2C12 myoblast alignment is important in obtaining highly aligned C2C12 myotubes because myoblasts fuse together in an end-to-end direction to form myotubes and myotube alignment is crucial to maximize the contractility and force generation within muscle tissues.[30] Therefore, we created a groove-ridge micropattern on the GelMA hydrogels, as shown in **Figure 4**-A, to make 3D myofibers within the grooves. The C2C12 myotubes were subjected to electrical stimulation (ES) (voltage 8 V, frequency 1 Hz, and duration 10 ms) at day 8 of culture for 2 continuous days. C2C12 myotubes cultured in the absence of ES were used as control samples. Differentiation of C2C12 myoblasts on GelMA-aligned CNT micropatterns due to the ES was confirmed by fluorescent staining of myosin heavy chain and α-actin proteins at day 10 of culture (Figure 4-B and 4-C) as a standard measure

ADVANCED MATERIALS
www.advmat.de

www.MaterialsViews.com

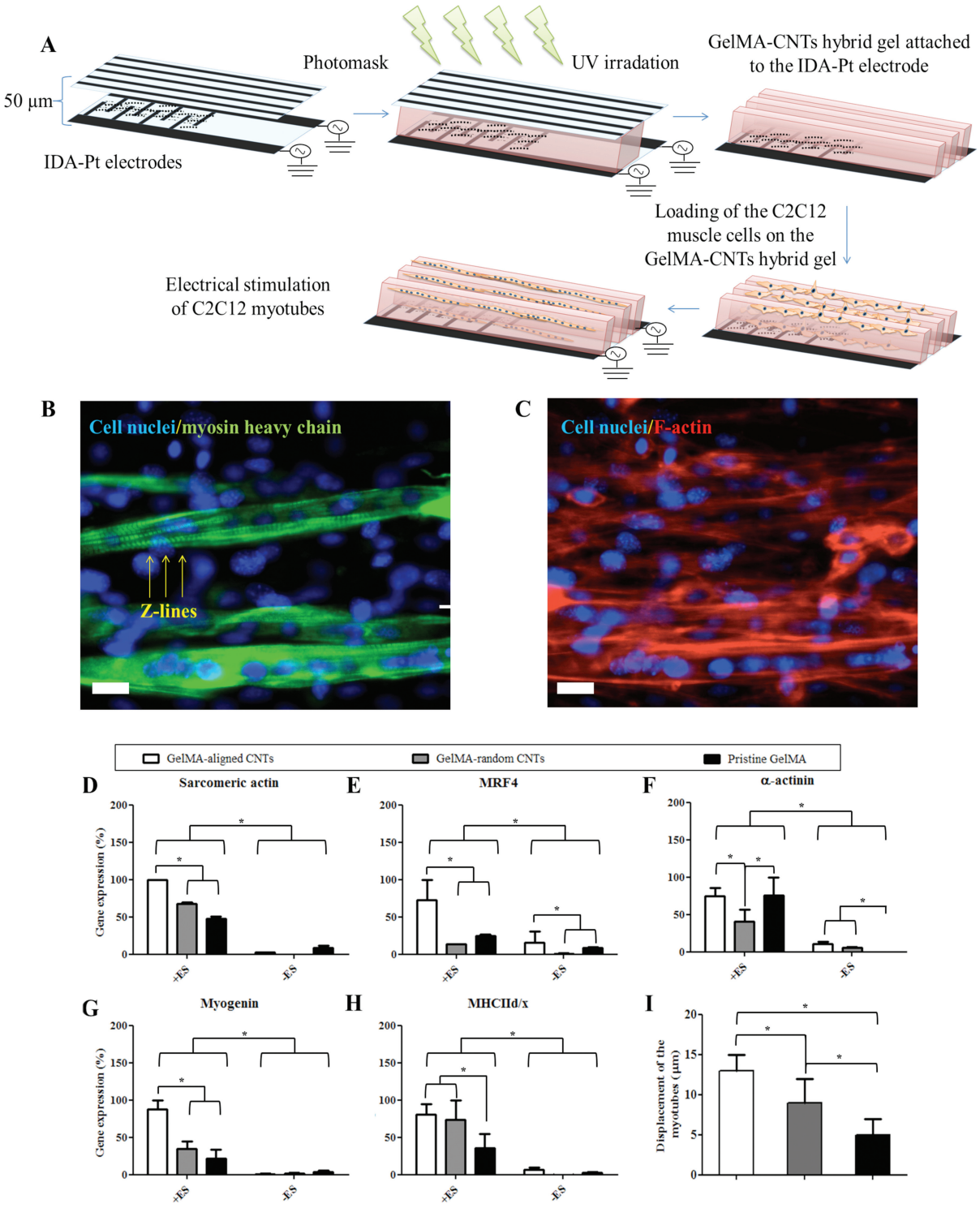

Figure 4. CNT alignment within GelMA hydrogel and differentiation of C2C12 myoblasts on the obtained GelMA-CNT hydrogel. (A) Schematic representation of the procedure to fabricate a groove-ridge topography within the GelMA-CNT hybrid gel (0.3 mg/mL CNTs). Immunostaining of cell nuclei/myosin heavy chain (B) and cell nuclei/F-actin (C). Gene expression analysis of fabricated muscle myofibers on GelMA and GelMA-CNT hydrogels with (+ES) or without (-ES) electrical stimulation at day 10 of culture. Expressions levels of (D) sarcomeric actin, (E) MRF4, (F) α-actinin, (G) myogenin, and (H) MHCIId/x in fabricated muscle myofibers grown on the pristine GelMA, aligned CNTs within the GelMA hydrogel (0.3 mg/mL CNTs), and random CNTs within the GelMA (0.3 mg/mL). (I) Displacements of myotubes due to ES on the pristine GelMA, aligned CNTs within the GelMA hydrogel (0.3 mg/mL CNTs) and random CNTs within the GelMA (0.3 mg/mL). ES was applied at day 8 of culture with a voltage 8 V, a frequency 1 Hz, and a duration of 10 ms for 2 continuous days. Scale bars are 50 μm. The expression levels of genes were normalized with respect to the internal reference gene GAPDH. Asterisks indicate significant differences between samples ($*p < 0.05$).

of myotube formation and contraction.[32] Figure 4-D to 4-H show the gene expression of fabricated muscle myofibers that were cultured on pristine GelMA or on GelMA containing randomly oriented CNTs or aligned CNTs with/without applying ES. Myogenin and MRF4 genes are responsible for the interaction with the muscle LIM protein during muscle maturation and are highly expressed in mature adult skeletal muscles.[33] Sarcomeric actin, α-actinin, and myosin heavy chain isofactor IId/x (MHCIId/x) are contraction-related genes and are expressed as a result of sarcomeric development within the muscles. Most importantly, gene analysis revealed that ES substantially promoted muscle cell differentiation and contraction, and this effect was more profound for C2C12 myotubes cultured on GelMA hydrogels with aligned CNTs compared with C2C12 myotubes cultured on pristine GelMA or on GelMA hydrogels with randomly dispersed CNTs. This difference is mainly attributed to the higher conductivity of aligned CNTs in the GelMA along with the CNT alignment compared with the other hydrogels. CNTs were patterned parallel to the electric field and therefore increased the efficiency of ES. Contraction of the stimulated myotubes was also observed and recorded (Movies S2-S4 and Figure 4-I). Electrically stimulated myotubes cultured on GelMA hydrogels with aligned CNTs exhibited more displacement compared with those cultured on pristine GelMA or on GelMA hydrogels with randomly dispersed CNTs. Other studies have confirmed a major role of scaffold conductivity on muscle cell differentiation and contraction. For example, poly(ε-caprolactone) (PCL), PCL-MWCNTs, and PCL-MWCNTs have been combined with polyvinyl alcohol and polyacrylic acid (abbreviated by authors as PCL-MWCNTs-H) as the scaffolds for skeletal muscle tissue engineering.[34] MWCNTs increase the conductivity of scaffolds. However, only PCL-MWCNTs-H scaffolds with the highest conductivity show contraction upon applying an electric field. Myotube formation is also improved on latter scaffolds compared with the PCL and PCL-MWCNT scaffolds.

In summary, DEP was proposed to achieve highly aligned CNTs within GelMA hydrogels in a facile and rapid way. This method is universal to make any type of CNTs micropatterns inside the biological scaffolds for various biological applications. Anisotropically aligned GelMA-CNT hydrogels showed higher conductivity compared with randomly distributed CNTs in the GelMA hydrogel and the pristine GelMA hydrogel. Due to the high electrical conductivity of aligned GelMA-CNT hydrogels, the engineered myofibers cultivated on these materials demonstrated more maturation and contractility, particularly after applying ES along with the CNT alignment, compared with the corresponding muscle myofibers cultured on pristine GelMA or GelMA hydrogels with randomly distributed CNTs. GelMA-CNTs hydrogels with tunable mechanical and electrical properties may be used in biosensing, development of hybrid 3D electronics-tissue materials, and for engineering functional tissues for various other applications.

Supporting Information

Experimental section, Figure S1-S6, Table S1, and Movies S1-S4.

Acknowledgements

The authors acknowledge Dr. Masatomo Sumiya and Mickael Lozac'h (NIMS) for providing the *I–V* measurement system. S. A., A. K., and J. R.-A. conceived the idea and designed the research. M. E. functionalized the CNTs; prepared their aqueous solutions; and performed the conductivity and zeta potential measurements, Raman spectroscopy, and TEM and SEM observations for the CNTs under supervision of Y. S. X. L. helped with the AFM measurements under supervision of K. N. S. O. synthesized the GelMA prepolymer. S. A. and J. R.-A. performed all other experiments, analyzed the results, contributed equally to the work, and wrote the paper. H. K., H. S., M. R., A. K., and T. M. supervised the research. All authors read the manuscript, provided comments, and approved its content. This work was supported by the World Premier International Research Center Initiative (WPI), MEXT, Japan.

Received: March 22, 2013
Revised: May 7, 2013
Published online: June 25, 2013

[1] B. V. Slaughter, S. S. Khurshid, O. Z. Fisher, A. Khademhosseini, N. A. Peppas, *Adv. Mater.* **2009**, *21*, 3307.
[2] N. A. Peppas, J. Z. Hilt, A. Khademhosseini, R. Langer, *Adv. Mater.* **2006**, *18*, 1345.
[3] T. Dvir, B. P. Timko, M. D. Brigham, S. R. Naik, S. S. Karajanagi, O. Levy, H. Jin, K. K. Parker, R. Langer, D. S. Kohane, *Nat. Nanotechnol.* **2011**, *6*, 720.
[4] L. Xu, Z. Jiang, Q. Qing, L. Mai, Q. Zhang, C. M. Lieber, *Nano Lett.* **2012**, *13*, 746.
[5] B. Tian, J. Liu, T. Dvir, L. Jin, J. H. Tsui, Q. Qing, Z. Suo, R. Langer, D. S. Kohane, C. M. Lieber, *Nat. Mater.* **2012**, *11*, 986.
[6] P. Schwille, *Science.* **2011**, *333*, 1252.
[7] K. T. Sapra, H. Bayley, *Sci. Rep.* **2012**, *2*, 848.
[8] S. R. Shin, S. M. Jung, M. Zalabany, K. Kim, P. Zorlutuna, S. Kim, M. Nikkhah, M. Khabiry, M. Azize, J. Kong, K. Wan, T. Palacios, M. R. Dokmeci, H. Bae, X. Tang, A. Khademhosseini, *ACS Nano* **2013**, *7*, 2369.
[9] T. Dvir, B. P. Timko, D. S. Kohane, R. Langer, *Nat. Nanotechnol.* **2011**, *6*, 13.
[10] J.-O. You, M. Rafat, G. J. C. Ye, D. T. Auguste, *Nano Lett.* **2011**, *11*, 3643.
[11] T. Cohen-Karni, R. Langer, D. S. Kohane, *ACS Nano* **2012**, *6*, 6541.
[12] F. J. Rawson, C. L. Yeung, S. K. Jackson, P. M. Mendes, *Nano Lett.* **2012**, *13*, 1.
[13] A. K. Shalek, J. T. Gaublomme, L. Wang, N. Yosef, N. Chevrier, M. S. Andersen, J. T. Robinson, N. Pochet, D. Neuberg, R. S. Gertner, I. Amit, J. R. Brown, N. Hacohen, A. Regev, C. J. Wu, H. Park, *Nano Lett.* **2012**, *12*, 6498.
[14] J. W. Nichol, S. T. Koshy, H. Bae, C. M. Hwang, S. Yamanlar, A. Khademhosseini, *Biomaterials* **2010**, *31*, 5536.
[15] S. R. Shin, H. Bae, J. M. Cha, J. Y. Mun, Y.-C. Chen, H. Tekin, H. Shin, S. Farshchi, M. R. Dokmeci, S. Tang, A. Khademhosseini, *ACS Nano* **2012**, *6*, 362.
[16] J. Ramón-Azcón, T. Yasukawa, H. J. Lee, T. Matsue, F. Sánchez-Baeza, M.-P. Marco, F. Mizutani, *Biosens. Bioelectron.* **2010**, *25*, 1928.
[17] J. Ramón-Azcón, R. Kunikata, F.-J. Sanchez, M.-P. Marco, H. Shiku, T. Yasukawa, T. Matsue, *Biosens. Bioelectron.* **2009**, *24*, 1592.
[18] J. H. Sung, H. S. Kim, H.-J. Jin, H. J. Choi, I.-J. Chin, *Macromolecules* **2004**, *37*, 9899.
[19] J. Ayutsede, M. Gandhi, S. Sukigara, H. Ye, C. Hsu, Y. Gogotsi, F. Ko, *Biomacromolecules* **2005**, *7*, 208.
[20] R. Sen, B. Zhao, D. Perea, M. E. Itkis, H. Hu, J. Love, E. Bekyarova, R. C. Haddon, *Nano Lett.* **2004**, *4*, 459.

[21] Y. Dror, W. Salalha, R. L. Khalfin, Y. Cohen, A. L. Yarin, E. Zussman, *Langmuir* **2003**, *19*, 7012.
[22] F. Ko, Y. Gogotsi, A. Ali, N. Naguib, H. Ye, G. L. Yang, C. Li, P. Willis, *Adv. Mater.* **2003**, *15*, 1161.
[23] C. M. Voge, M. Kariolis, R. A. MacDonald, J. P. Stegemann, *J. Biomed. Mater. Res. Part A.* **2008**, *86A*, 269.
[24] S. Namgung, K. Y. Baik, J. Park, S. Hong, *ACS Nano* **2011**, *5*, 7383.
[25] B. V. Derjaguin, V. M. Muller, Y. Toporov, *J. Coll. Interf. Sci.* **1975**, *53*, 314.
[26] G. C. Reilly, A. J. Engler, *J. Biomech.* **2010**, *43*, 55.
[27] M. P. Lutolf, P. M. Gilbert, H. M. Blau, *Nature* **2009**, *462*, 433.
[28] H. Aubin, J. W. Nichol, C. B. Hutson, H. Bae, A. L. Sieminski, D. M. Cropek, P. Akhyari, A. Khademhosseini, *Biomaterials* **2010**, *31*, 6941.
[29] J. Suhr, N. Koratkar, P. Keblinski, P. Ajayan, *Nat. Mater.* **2005**, *4*, 134.
[30] a) V. Hosseini, S. Ahadian, S. Ostrovidov, G. Camci-Unal, S. Chen, H. Kaji, M. Ramalingam, A. Khademhosseini, *Tissue Eng. Pt. A.* **2012**, *18*, 2453; b) S. Ahadian, J. Ramon-Azcon, S. Ostrovidov, G. Camci-Unal, H. Kaji, K. Ino, H. Shiku, A. Khademhosseini, T. Matsue, *Lab Chip* **2012**, *12*, 3491; c) S. Ahadian, S. Ostrovidov, V. Hosseini, H. Kaji, M. Ramalingam, H. Bae, A. Khademhosseini, *Organogenesis* **2013**, *9*, April/May/June 2013.
[31] J. Ramon-Azcon, S. Ahadian, R. Obregon, G. Camci-Unal, S. Ostrovidov, V. Hosseini, H. Kaji, K. Ino, H. Shiku, A. Khademhosseini, T. Matsue, *Lab Chip* **2012**, *12*, 2959.
[32] S. Ahadian, J. Ramon-Azcon, S. Ostrovidov, G. Camci-Unal, V. Hosseini, H. Kaji, K. Ino, H. Shiku, A. Khademhosseini, T. Matsue, *Lab Chip* **2012**, *12*, 3491.
[33] S. Arber, G. Halder, P. Caroni, *Cell* **1994**, *79*, 221.
[34] S. Sirivisoot, B. Harrison, *Int. J. Nanomed.* **2011**, *6*, 2483.